# 41. MAGNETIC PROPERTIES OF IGNEOUS ROCKS OF THE PHILIPPINE SEA, DEEP SEA DRILLING PROJECT LEG 58

T. Furuta and K. Kobayashi, Ocean Research Institute, University of Tokyo
and
K. Momose, Department of Geology, Shinshu University, Matsumoto, Japan

## ABSTRACT

The Curie temperature and thermomagnetic behavior of whole-rock samples were measured in basalts recovered from Sites 442, 443, and 444 of DSDP Leg 58 in the Shikoku Basin, and from Site 446 in the Daito Basin, north Philippine Sea. Chemical composition and microscopic features of opaque oxides in the same samples were also investigated. Degree and mode of oxidation of titanomagnetite vary irrespective of site, lithology, or magnetic polarity, and no systematic correlation has been found between any two of these characteristics. Magnetic properties are systematically different between massive flows recovered at Hole 444A (Shikoku Basin) and Hole 446A (Daito Basin), although the controlling factor is unknown.

## INTRODUCTION

Alternating sequences of normal and reversed magnetic polarity were found in basaltic layers at Sites 442, 443, and 446 of Leg 58. At Site 444, the entire basalt sequence penetrated by drilling (~60 m) is reversely magnetized, opposite to the positive magnetic anomaly at this site, attributed to normal magnetization of rocks below the depth of penetration (see Site reports, this volume). In this paper, the correlation between magnetic polarity and degree of oxidation has been carefully examined in view of the possible origin of reversed magnetization by self-reversal.

Pillow basalts occur at Sites 442 and 443, while basalts at the other sites and those overlying and intercalated with the pillows are massive flows. Some massive basalts were identified as sills or sheets intruded into sediments. Possible differences in mineralogy of iron oxides between pillow and massive basalts—such as titanium content and degree of oxidation—have been extensively investigated.

## THERMOMAGNETIC MEASUREMENTS

Thermal changes in saturation magnetization, $J_s$, were measured on 28 samples from Site 442, 27 samples from Site 443, 10 samples from Site 444, and 42 samples from Site 446. A small chunk of rock (~100 mgs) was heated at 6°C/min in a magnetic field of approximately 4300 oe after the sample was heated at 620°C for 30 minutes, it was cooled to room temperature at the same rate. The cycle of heating and cooling was accomplished in a vacuum of $10^{-4}$ torr.

Two types of thermomagnetic curves were recognized: thermally reversible (Figure 1a) and irreversible types (Figures 1b–d); both types are normally found among submarine basalts. In the reversible samples, the Curie temperature ($T_{c1}$) is easily determined, as shown in Figure 1a. The Curie temperature markedly decreases in some samples (e.g., 442B-8-1, 444-27-1) after heating at 620°C. (The Curie temperature after heating at 620°C is denoted by $T_{ch}$).

With irreversible curves, more than two Curie temperatures, ($T_{c1}$, $T_{c2}$, $T_{c3}$,.... $T_{ci}$) can be distinguished. The Curie temperature revealed in the cooling process is usually that which is nearly the same or slightly lower than the highest $T_{ci}$ seen in the heating process. It has been concluded that the recognition of more than two Curie temperatures in the heating process is not due to coexistence of multiple magnetic phases in the original rock, but is caused by stepwise inversion of titanomaghemite (spinel-cubic form of titanomagnetite oxidized at a low temperature) to less-titaniferous magnetite at higher temperatures (Ozima et al., 1968; Ozima and Larson, 1970). The Curie temperature of less-titaniferous magnetite is higher than that of magnetite richer in titanium (Akimoto and Katsura, 1959).

Ratios of intensities of saturation magnetization at room temperature before and after heating at 620°C, ($J_{ho}/J_o$) were calculated from the thermomagnetic measurements and are listed in Table 1. The ratio varies from 0.5 to 4.0, but most frequently has values of around 1.0 in the samples investigated. These values are listed in Table 1 together with the Curie temperatures.

## MICROSCOPY OF OPAQUE MINERALS

Opaque minerals were examined in polished sections by reflected-light microscopy. Titanomagnetite was distinguished from ilmenite by its color and anisotropy, and from sulfide by its color. The majority of titanomagnetite and titanomaghemite grains are optically uniform, as seen in Figure 2a,c. Some titanomagnetites have well-developed cracks (Figure 2d), similar to those reported by Hall et al. (1976), Johnson and Hall (1978), and Kobayashi et al. (1979). Figure 2e shows titanomag-

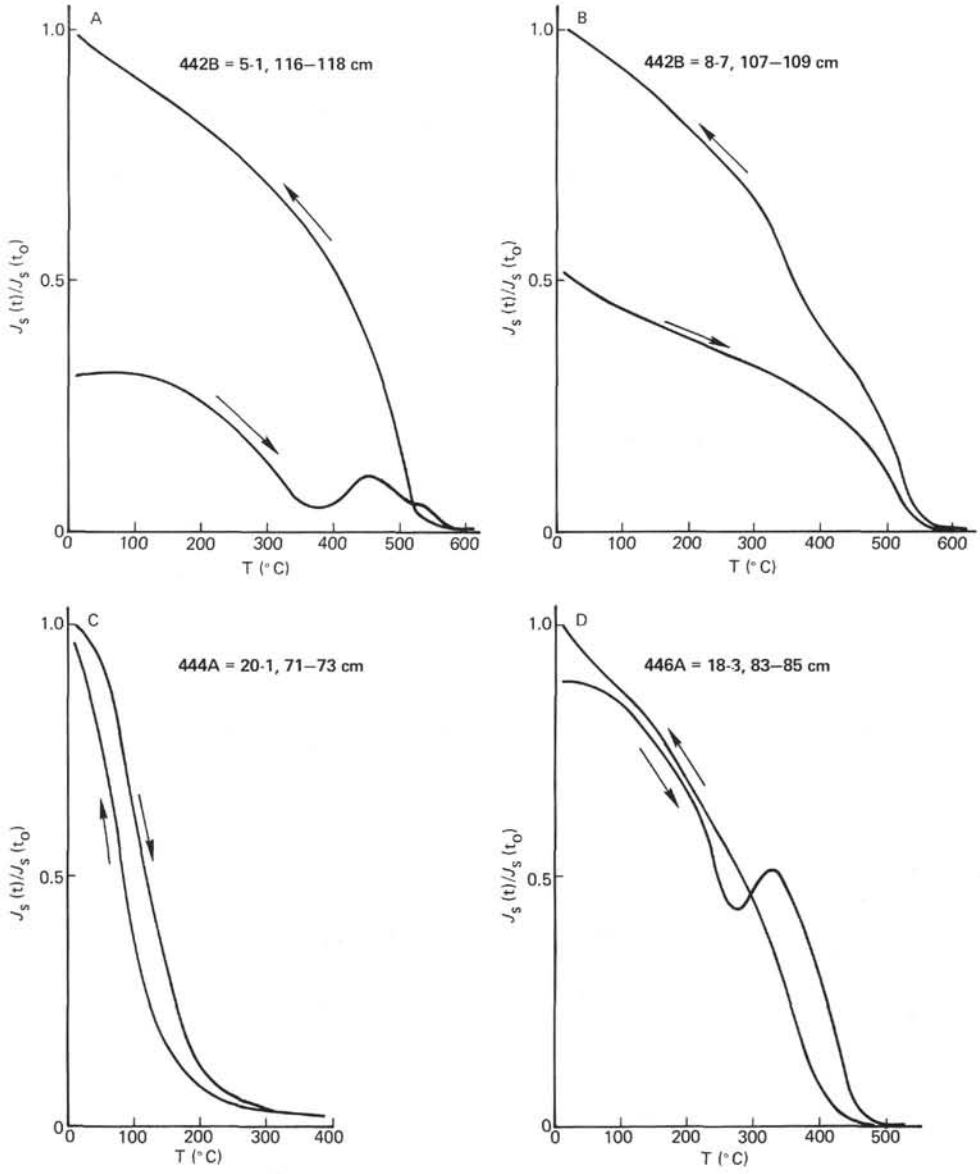


Figure 1. *Thermomagnetic curves of typical samples (*H = *4300 oe;* P = $10^{-4}$ *torr).* A. *Thermally irreversible type, typical of submarine basalts; 442B-5-1, 116–118 cm.* B. *Thermally reversible type, with evidence of high-temperature oxidation; 442B-8-7, 107–109 cm.* C. *Thermally reversible type, unoxidized sample; 444A-20-1, 71–73 cm.* D. *Thermally irreversible type, common in Hole 446A; 446A-18-3, 83–85 cm.*

netite containing ilmenite exsolution lamellae along {111} planes. Figure 2f shows a skeletal grain of titanomagnetite which appears to have been oxidized at a high temperature.

## ELECTRON-MICROPROBE ANALYSIS OF OPAQUE MINERALS

The Ti/Fe ratio in titanomagnetite and ilmenite, if the grain size is larger than 10$\mu$m, was determined by a JXA-5 electron-probe microanalyzer. The composition was determined in more than 20 grains of one specimen, and the results were averaged, although intergrain scatter is generally small.

The molecular percentage of Ti to Fe is shown in Table 1. The contents of other elements were measured in the same grains. Figure 3 shows concentration profiles across a grain of titanomagnetite. It is recognized that the $TiO_2$ content is roughly proportional to that of FeO, while that of $Al_2O_3$ is inversely proportional to that of FeO and $TiO_2$. Contents of MnO, MgO, and $V_2O_3$ are less than 1 weight per cent in all tested titanomagnetite grains. The $Al_2O_3$ content ranges from 0.7 to

TABLE 1
Summary of Magnetic Properties and Chemical Composition of Opaque Minerals in DSDP Leg 58 Basaltic Samples

| Sample (interval in cm) | Type[a] | Curie Temperature ($T_{c1}$ | $T_{c2}$ | $T_{c3}$ | $T_{ch}$ (°C)) | $J_{ho}/J_o$ | Titanomagnetite Ti/Fe (based on mol %) | $x$ Value[b] | $Al_2O_3$ (wt. %) | Size (μm) | Ilmenite Ti/Fe (based on mol %) | Remarks | Rock Texture[c] |
|---|---|---|---|---|---|---|---|---|---|---|---|---|---|
| 442B-3-3, 118-120 | I | 295 | 525 | 555 | 530 | 3.2 | | | | | | | |
| 4-1, 117-119 | I | 410 | 555 | 570 | 535 | 3.1 | 21.8 | 0.537 | 2.7 | 30-50 | – | – | pl-cpx hyalo-ophitic basalt |
| 5-1, 116-118 | I | 360 | 540 | 560 | 525 | 3.0 | 26.8 | 0.633 | 2.6 | 10-20 | – | – | pl-cpx subophitic dolerite |
| 6-1, 48-50 | I | 390 | 540 | 570 | 530 | 3.2 | – | – | – | 10 | – | – | pl-cpx hyalo-ophitic basalt |
| 6-2, 110-112 | I | 470 | – | 565 | 545 | 1.8 | – | – | – | 10-20 | – | – | pl-cpx hyalo-ophitic basalt |
| 7-1, 59-61 | (R) | 345 | 440 | – | 370 | 1.1 | – | – | – | – | – | – | – |
| 7-1, 106-108 | (R) | 270 | – | – | 360 | 1.2 | 26.2 | 0.633 | 1.2 | 200-300 | – | – | pl-cpx subophitic dolerite |
| 8-1, 47-49 | R | 300 | – | – | 245 | 0.9 | 23.9 | 0.579 | 1.1 | 150-200 | – | – | pl-cpx subophitic dolerite |
| 8-2, 24-26 | (R) | 365 | – | – | 285 | 0.95 | – | – | – | – | – | – | – |
| 8-3, 55-57 | R | 470 | – | – | 410 | 0.9 | 24.2 | 0.585 | 1.4 | 300-400 | – | Il lamella | pl-cpx subophitic dolerite |
| 8-5, 23-25 | R | 250 | – | – | 195 | 0.95 | 23.9 | 0.580 | 1.7 | 100-200 | 86.4 | – | pl-cpx subophitic dolerite |
| 8-6, 84-86 | R | 205 | – | – | 200 | 1.0 | – | – | – | – | – | – | – |
| 8-7, 107-109 | (R) | 550 | – | – | 535 | 0.5 | 29.4 | 0.706 | 0.7 | 200 | 82.9 | Il lamella | pl-cpx subophitic dolerite |
| 9-1, 24-26 | (R) | 570 | – | – | 550 | 2.3 | 32.4 | 0.734 | 1.1 | 150-200 | 95.4 | – | pl-cpx subophitic dolerite |
| 9-1, 33-35 | (R) | 570 | – | – | 550 | 2.1 | – | – | – | – | – | – | – |
| 9-1, 103-105 | (R) | 450 | – | 590 | 550 | 1.5 | 25.5 | 0.610 | 1.2 | 100 | 99.0 | – | pl-cpx intersertal basalt |
| 9-2, 73-75 | I | – | – | 550 | 525 | 2.6 | – | – | – | – | – | – | – |
| 9-3, 32-34 | I | 390 | 550 | 570 | 490 | 3.1 | – | – | – | – | – | – | – |
| 11-1, 60-62 | I | 365 | 555 | 560 | 535 | 4.2 | – | – | – | <10 | – | Sulfide | pl-cpx intersertal basalt |
| 11-3, 18-20 | I | 335 | 525 | 555 | 525 | 3.4 | – | – | – | <10 | – | – | pl-cpx intersertal basalt |
| 13-1, 60-62 | I | 315 | 520 | 580 | 530 | 3.6 | – | – | – | – | – | – | – |
| 13-3, 2-4 | I | 380 | 550 | 560 | 530 | 3.8 | – | – | – | – | – | – | – |
| 16-1, 29-31 | I | 250 | 535 | 580 | 510 | 2.7 | 25.7 | 0.614 | 2.0 | 30-40 | – | – | pl-cpx intersertal basalt |
| 16-1, 34-36 | I | 285 | 550 | 570 | 530 | 3.6 | 24.9 | 0.599 | 2.1 | 50-70 | – | – | pl-cpx intersertal basalt |
| 16-2, 24-26 | I | 340 | – | 580 | 545 | 5.1 | – | – | – | 70 | – | – | pl-cpx hyalo-ophitic basalt |
| 17-1, 104-106 | I | 440 | 535 | 555 | 530 | 3.4 | – | – | – | <5 | – | – | pl-cpx intersertal basalt |
| 19-2, 62-64 | I | 220 | 510 | – | 475 | 1.9 | – | – | – | 50-70 | – | – | pl-cpx hyalo-ophitic basalt |
| 20-1, 27-29 | I | 380 | 560 | 570 | 535 | 4.1 | – | – | – | 5-7 | – | – | pl-cpx intersertal basalt |
| 443-49-3, 137-139 | (I) | 210 | 310 | – | 525 | 1.9 | – | – | – | 300 | – | – | pl-cpx*-ol ophitic dolerite |
| 49-4, 102-104 | R | 155 | – | – | 230 | 1.1 | 28.4 | 0.663 | 1.0 | 300 | 91.6 | – | pl-cpx* ophitic dolerite |
| 50-2, 30-32 | (I) | 270 | – | – | 540 | 1.3 | – | – | – | 150 | – | – | pl-cpx* ophitic dolerite |
| 52-1, 33-35 | I | 325 | 490 | 540 | 560 | 3.6 | – | – | – | 90 | – | – | pl-cpx hyalo-ophitic basalt |
| 52-4, 21-23 | (R) | 145 | – | – | 210 | 1.2 | – | – | – | 300 | – | – | pl-cpx-ol hyalo-ophitic basalt |
| 53-2, 12-14 | I | 240 | 480 | 550 | 535 | 3.5 | – | – | – | 120 | – | – | pl-cpx hyalo-ophitic basalt |
| 54-2, 54-56 | R | 100 | – | – | 110 | 1.0 | – | – | – | 20 | – | – | pl-cpx-ol intersertal basalt |
| 54-3, 125-127 | I | 230 | 470 | – | 505 | 4.1 | 36.2 | 0.797 | – | 400 | 95.6 | – | pl-cpx-ol ophitic dolerite |
| 54-5, 146-148 | I | 290 | 570 | – | 560 | 5.2 | – | – | – | 3 | – | – | pl-cpx hyalo-ophitic basalt |
| 54-7, 76-78 | R | 105 | – | – | 140 | 1.0 | 27.7 | 0.650 | 1.6 | 30 | – | – | pl-cpx hyalo-ophitic basalt |
| 55-1, 99-101 | I | 315 | – | – | 535 | 3.2 | – | – | – | 10 | – | – | pl-cpx hyalo-ophitic basalt |
| 56-1, 117-119 | I | 390 | 560 | – | 570 | 4.4 | – | – | – | 10 | – | – | aphyric basalt |
| 56-3, 120-122 | I | 280 | 460 | 490 | 540 | 3.5 | – | – | – | 30 | – | – | pl-cpx intersertal basalt |
| 58-1, 61-63 | I | 410 | – | – | 555 | 2.0 | – | – | – | 30 | – | – | aphyric basalt |
| 58-3, 34-36 | (R) | 515 | – | – | 540 | – | – | – | – | 60 | – | – | pl-cpx intersertal basalt |
| 58-4, 6-8 | I | 240 | 410 | – | 460 | – | – | – | – | 150 | – | – | pl-cpx intersertal basalt |
| 443-59-2, 15-17 | I | 200 | 425 | – | 450 | 2.2 | – | – | – | 300 | – | – | pl-cpx-ol ophitic dolerite |
| 59-3, 12-14 | (I) | 170 | – | – | 500 | 1.5 | 29.9 | 0.691 | 1.5 | 150-300 | 84.2 | – | pl-cpx-ol ophitic dolerite |
| 60-1, 17-19 | R | 190 | – | – | 200 | 0.9 | 27.1 | 0.637 | 1.8 | 180 | 88.1 | – | pl-cpx ophitic dolerite |
| 60-2, 110-112 | I | 185 | 525 | – | 545 | 1.8 | – | – | – | 250 | – | – | pl-cpx-ol subophitic dolerite |
| 60-4, 125-127 | R | 125 | – | – | 160 | 1.0 | 29.0 | 0.674 | 1.5 | 420 | 92.0 | – | pl-cpx-ol ophitic dolerite |
| 61-2, 103-105 | I | 250 | 490 | – | 520 | – | – | – | – | 100-150 | – | – | pl-ol intersertal basalt |
| 62-1, 90-92 | I | 240 | 420 | – | 480 | 2.5 | – | – | – | 180 | – | – | pl-cpx intersertal basalt |
| 62-4, 62-64 | I | 270 | 515 | 575 | 560 | 4.1 | 27.9 | 0.654 | 2.2 | 10-30 | – | – | pl intersertal basalt |
| 63-2, 71-73 | I | 240 | 475 | – | 515 | 2.7 | – | – | – | 100-150 | – | – | pl-cpx subophitic dolerite |
| 63-5, 126-128 | I | 365 | 525 | 570 | 575 | 4.0 | – | – | – | 60 | – | – | pl-cpx subophitic dolerite |
| 63-8, 84-86 | R | 120 | – | – | 125 | 0.95 | 28.3 | 0.662 | – | 300 | 91.4 | – | pl-cpx-ol ophitic dolerite |
| 444A-20-1, 27-29 | R | 265 | – | – | 215 | 0.94 | 22.3 | 0.546 | 2.9 | 150 | 89.4 | – | pl-ol-cpx*-ka ophitic dolerite |
| 20-1, 71-73 | R | 180 | – | – | 140 | 0.96 | 25.9 | 0.617 | 2.3 | 150 | 92.2 | – | pl-ol-cpx*-ka ophitic dolerite |
| 20-4, 46-48 | R | 235 | – | – | 200 | 0.95 | – | – | – | – | – | – | – |
| 23-2, 87-89 | R | 250 | – | – | 205 | 0.94 | 24.3 | 0.586 | 1.6 | 100 | – | – | pl-cpx-ol subophitic dolerite |
| 23-2, 138-140 | R | 310 | 450 | – | 300 | 1.03 | – | – | – | 150 | – | – | pl-cpx ophitic dolerite |
| 25-1, 49-51 | R | 445 | – | – | 275 | 0.95 | – | – | – | 500 | – | Il lamella | pl-cpx ophitic dolerite |
| 25-3, 92-94 | R | 460 | – | – | – | 0.92 | – | – | – | 200 | – | Il lamella | pl-cpx ophitic dolerite |
| 26-2, 5-7 | R | 185 | – | – | 120 | 0.88 | 28.8 | 0.670 | 4.1 | 500 | – | – | pl-cpx-ol ophitic dolerite |
| 27-1, 90-92 | R | 425 | – | – | 210 | 0.91 | 24.2 | 0.585 | 1.8 | 300 | – | Il-rich | pl-cpx-ol ophitic dolerite |
| 27-5, 39-41 | R | 290 | – | – | 160 | 0.92 | – | – | – | 200 | – | – | pl-cpx-ol subophitic dolerite |
| 446A-2-1, 145-147 | I | 250 | 455 | – | 365 | 1.5 | – | – | – | 70-100 | – | – | pl-cpx*-ka subophitic dolerite |
| 2-3, 41-43 | (I) | 435 | – | – | 260 | 0.8 | – | – | – | <10 | – | Sulfide-rich | aphyric basalt |
| 3-3, 50-52 | I | 230 | 460 | – | 400 | 1.0 | – | – | – | – | – | – | – |
| 3-4, 34-36 | R | 240 | – | – | 200 | 0.8 | – | – | – | – | – | – | – |
| 4-1, 32-34 | R | 245 | – | – | 230 | 0.9 | 26.5 | 0.628 | 2.1 | 150-200 | 88.1 | – | pl-cpx*-ka subophitic dolerite |

TABLE 1 – *Continued*

| Sample (interval in cm) | Type[a] | Curie Temperature $T_{c1}$ (°C) | $T_{c2}$ (°C) | $T_{c3}$ (°C) | $T_{ch}$ (°C) | $J_{ho}/J_o$ | Titanomagnetite Ti/Fe (based on mol %) | $x$ Value[b] | $Al_2O_3$ (wt. %) | Size (μm) | Ilmenite Ti/Fe (based on mol %) | Remarks | Rock Texture[c] |
|---|---|---|---|---|---|---|---|---|---|---|---|---|---|
| 446A-19-2, 14-16 | (I) | 505 | – | – | 440 | 0.9 | – | – | – | – | – | – | – |
| 19-5, 18-20 | I | 390 | 460 | – | 405 | 1.0 | – | – | – | 20-30 | – | – | pl-cpx hyalo-ophitic basalt |
| 20-3, 140-142 | I | – | 470 | – | 445 | 1.1 | – | – | – | – | – | – | – |
| 21-1, 82-84 | I | 315 | 440 | – | 415 | 1.1 | – | – | – | – | – | – | – |
| 21-3, 79-81 | I | 365 | 450 | – | 410 | 1.15 | – | – | – | – | – | – | – |
| 21-6, 16-18 | I | 370 | 455 | – | 440 | 1.1 | – | – | – | – | – | – | – |
| 22-1, 145-147 | (I) | 405 | 460 | – | 435 | 0.9 | 22.6 | 0.554 | 3.1 | 100 | 79.6 | – | pl-cpx intersertal basalt |
| 22-4, 95-97 | (I) | 390 | 455 | – | 410 | 1.0 | 22.0 | 0.541 | 3.1 | 100-200 | 76.3 | – | pl-cpx intersertal basalt |
| 23-2, 43-45 | (I) | 460 | – | – | 365 | 0.9 | 17.1 | 0.437 | 2.5 | 40-60 | 74.1 | – | pl-cpx*-ka intersertal basalt |
| 23-6, 101-103 | (I) | 465 | – | – | 425 | 1.0 | 25.0 | 0.604 | 1.9 | 100-150 | 84.5 | – | pl-cpx subophitic dolerite |
| 24-1, 43-45 | I | 290 | 455 | – | 430 | 1.4 | 34.4 | 0.768 | 2.8 | 10-30 | – | Il-rich | pl-cpx intersertal basalt |
| 25-1, 13-15 | R | 290 | – | – | 215 | 0.9 | – | – | – | – | – | – | – |
| 25-3, 41-43 | (I) | 410 | 455 | – | 385 | 0.9 | – | – | – | – | – | – | – |
| 26-3, 44-46 | I | 305 | 435 | – | 400 | 1.0 | – | – | – | – | – | – | – |
| 26-3, 142-144 | I | 315 | 425 | – | 475 | 1.3 | 23.4 | 0.569 | 2.2 | 70-100 | 79.2 | – | pl-cpx ophitic dolerite |
| 27-1, 77-79 | I | 290 | 455 | – | 420 | 1.2 | – | – | – | 10-20 | – | – | pl intersertal basalt |
| 28-1, 100-102 | (I) | 380 | 450 | – | 360 | 0.9 | – | – | – | 15-20 | – | – | pl intersertal basalt |
| 4-2, 44-46 | I | 280 | 440 | – | 415 | 1.3 | 20.6 | 0.512 | 4.6 | 80-100 | 85.7 | – | pl-cpx*-ka subophitic dolerite |
| 5-1, 16-18 | I | 260 | 420 | – | 370 | 1.2 | – | – | – | – | – | – | – |
| 5-2, 24-26 | I | 280 | 450 | – | 430 | 1.3 | – | – | – | – | – | – | – |
| 6-1, 10-12 | I | 300 | 470 | – | 440 | 1.4 | – | – | – | 80-100 | – | – | pl-cpx*-ka ophitic dolerite |
| 6-3, 109-111 | I | 280 | 445 | – | 430 | 1.2 | 28.2 | 0.659 | 3.0 | 100-150 | 86.0 | – | pl-cpx subophitic dolerite |
| 7-4, 138-140 | I | 285 | 440 | – | 425 | 1.2 | 24.2 | 0.585 | 2.9 | 100-200 | 79.0 | – | pl-cpx*-ka subophitic dolerite |
| 9-1, 82-84 | I | 290 | 440 | – | 430 | 1.2 | 27.8 | 0.653 | 2.6 | 50-100 | 84.2 | – | pl-cpx intersertal basalt |
| 10-5, 110-112 | (I) | 445 | 510 | – | 520 | 0.9 | – | – | – | – | – | – | – |
| 11-1, 69-71 | (I) | 510 | 545 | – | 465 | 0.9 | – | – | – | 70-100 | – | – | pl-cpx*-ka subophitic dolerite |
| 11-2, 23-25 | (I) | 350 | 460 | – | 395 | 0.9 | 29.3 | 0.680 | 2.2 | 150-200 | 89.5 | – | pl-cpx dolerite ophitic |
| 12-1, 53-55 | (I) | 265 | 435 | – | – | 1.0 | – | – | – | – | – | – | – |
| 12-2, 69-71 | R | 280 | – | – | 220 | 0.9 | 25.4 | 0.608 | 3.9 | 150-200 | 96.6 | – | pl-cpx*-ka subophitic dolerite |
| 13-1, 107-109 | R | 150 | – | – | 70 | 1.0 | 27.6 | 0.649 | 5.8 | 70-100 | – | – | pl-cpx*-ka subophitic dolerite |
| 14-1, 102-104 | I | 400 | 465 | – | 435 | 1.0 | – | – | – | – | – | – | – |
| 14-3, 66-68 | (I) | 350 | 440 | – | 405 | 0.9 | – | – | – | – | – | – | – |
| 15-3, 58-60 | I | 310 | 445 | – | 410 | 1.0 | – | – | – | 50-70 | – | – | pl intersertal basalt |
| 16-2, 44-46 | I | 310 | 445 | – | 395 | 1.0 | – | – | – | – | – | – | – |
| 17, CC | (I) | 515 | – | – | 500 | 0.8 | – | – | – | – | – | – | – |
| 18-3, 83-85 | I | 350 | 450 | – | 415 | 1.1 | – | – | – | 30-50 | – | Il-rich | pl-cpx intersertal basalt |
| 19-1, 69-71 | I | – | 495 | – | 455 | 1.0 | – | – | – | 150-200 | – | – | pl-cpx intersertal basalt |

[a]R = reversible; I = irreversible; parentheses indicate atypical curve.
[b]Value in the formula $x\ Fe_2TiO_4 \cdot (1-x)\ Fe_3O_4$.
[c]cpx* denotes titanaugite; ka denotes kaersutite.

5.8 (Table 1); its presence would slightly modify the $x$ value of titanomagnetite, if it occurs in a solid solution of magnetite–ulvospinel.

## RESULTS OF MEASUREMENTS

### Hole 442B

Basalt in this hole is present in upper and lower layers, with an intercalated 3-m-thick sediment layer. The upper layer consists only of massive flows; most of the lower layer is pillow flows, but these are intruded by two massive flows. These rocks are all olivine-depleted plagioclase–clinopyroxene basalts or dolerites.

The upper half of the upper massive-flow unit has irreversible thermomagnetic properties, with an initial Curie temperature ($T_{c1}$) ranging between 300 and 470°C. Most samples from the lower half of the upper massive-flow unit are reversible in a heating–cooling cycle, although some samples taken near the contacts with sediments are irreversible. Both pillows and massive flows in the lower part of the hole are thermomagnetically irreversible.

The molecular ratio of titanium to total iron in titanomagnetite was determined mostly in the upper, massive basalts, because the grains of opaque minerals are too small in the pillow lavas. The values obtained are 21.8 to 32.4 (corresponding to $x = 0.54$ to 0.73).

The initial Curie temperature ($T_{c1}$) of the thermally reversible samples ranges between 205 and 470°C, while the $x$ value is concentrated around 0.6 (0.58–0.63). These results are summarized in Table 1 and Figure 4. The Curie temperature of stoichiometric titanomagnetite with a composition of $x = 0.6$ is about 200°C (Akimoto et al., 1957; Ozima and Sakamoto, 1971), which is roughly consistent with the observed values in two samples (442B-8-5 and 442B-8-6). It is thus concluded that these two samples are unoxidized at low temperatures.

The observed Curie temperature for Sample 442B-8-3 is 470°C, although the measured $x$ value is 0.59. In Samples 442B-8-7, 24–26 cm and 442B-9-1, 33–35 cm, $T_{c1} = 520$ to 570°C, and $x = 0.71$ to 0.73. If the titanomagnetite is uniform and stoichiometric, the composition showing $T_{c1} = 470$°C is $x = 0.2$. Microscopic examination of polished sections revealed the occurrence of fine exsolution lamellae of ilmenite in the titanomagnetite of Samples 442B-8-3 and 442B-8-7. Exsolution may have been caused by high-temperature oxidation. The ilmenite lamellae are too fine to be analyzed by elec-

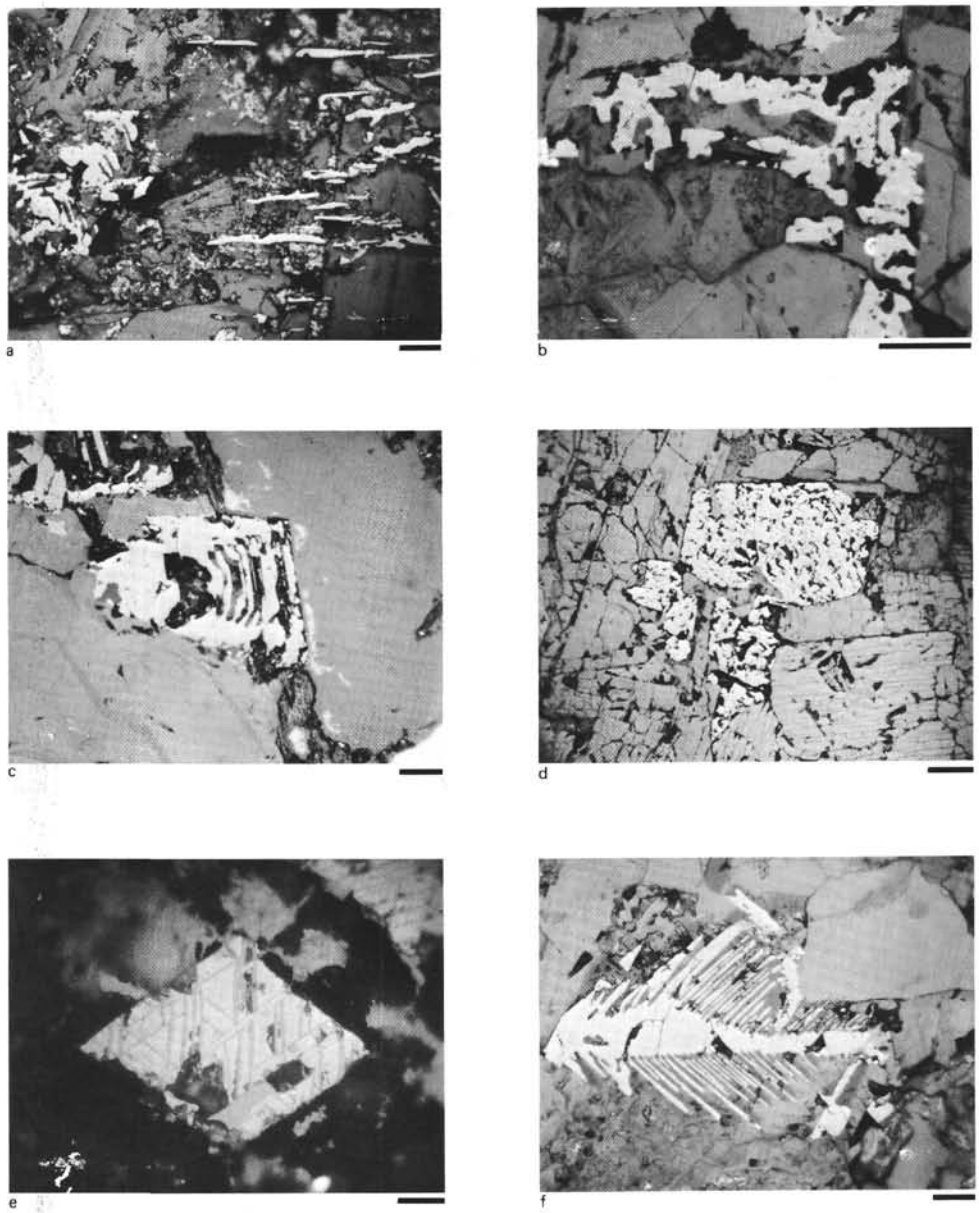

Figure 2. *Photomicrographs of typical opaque minerals in reflected light.* A. *Unoxidized titanomagnetite (left) and discrete grains of ilmenite (right); 442B-8-1, 47–49 cm; 50-μm scale.* B. *Titanomagnetite oxidized at a low temperature; 443-59-2, 15–17 cm; 50-μm scale.* C. *Unoxidized titanomagnetite; 442B-8-5, 23–25 cm; 50-μm scale.* D. *Unoxidized titanomagnetite with well-developed cracks; 444A-27-5, 39–41 cm; 100-μm scale.* E. *Magnetite with ilmenite exsolution lamellae along the {111} planes; 442B-8-7; 10-μm scale.* F. *Large skeletal grain of titanomagnetite oxidized at a low temperature; 442B-9-1, 24–25 cm; 50-μm scale.*

tron microprobe. The obtained content of titanium is probably the average of that in titanomagnetite and ilmenite. In some samples, discrete, idiomorphic ilmenite crystals are seen under the reflecting microscope. These ilmenite grains are sufficiently large for electron-microprobe analysis, and the molecular percentage of titanium was determined to be 83 to 99, which is close to stoichiometric ilmenite.

The initial Curie temperature of the thermally irreversible samples varies from 220 to 470°C. The $x$ value for Sample 442B-5-1, having $T_{cl} = 360$°C, is 0.63, and for Sample 442B-16-1, 29–31cm, having $T_{cl} = 250$°C, is 0.61. The ratio of saturation magnetization before and after heating at 620°C in a vacuum, $(J_{ho}/J_o)$ is 5.1 for Sample 442B-16-2, which may indicate a high degree of low-temperature oxidation of titanomagnetite.

**Hole 443**

More than seven massive flows and at least four pillow lavas were cored in this hole. The rocks are plagio-

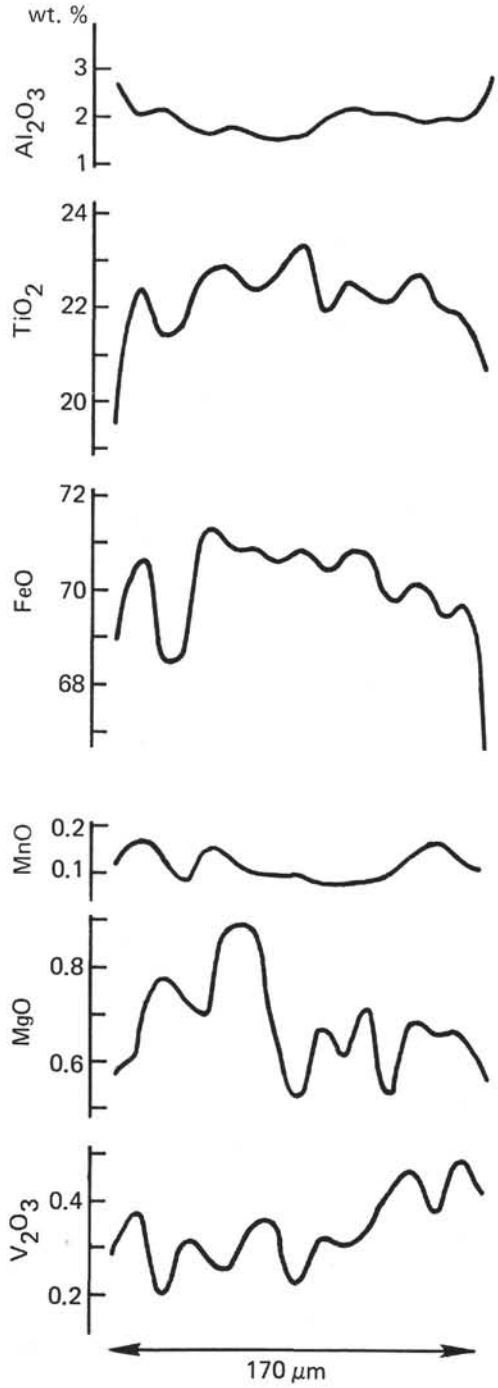


Figure 3. *Electron-microprobe profiles for principal oxides in one grain of titanomagnetite, Section 443-63-8. FeO represents* $\frac{2}{3}FeO + \frac{1}{3}Fe_2O_3$.

clase–clinopyroxene–olivine basalts and dolerites. Some contain titanaugite.

Some samples from the massive flows show thermally reversible magnetic properties, with Curie temperatures lower than 200°C. Sample 443-54-7, taken from a pillow lava, is also reversible, with a $T_{c1}$ = 105°C and a $T_{ch}$ = 140°C. Its $x$ value is 0.65, corresponding to a Curie temperature of about 130°C if the titanomagnetite is stoichiometric. The observed values of $T_{c1}$ and $x$ indicate that titanomagnetite in Sample 443-54-7 is completely unoxidized. A slight discrepancy between the observed and expected Curie temperatures may be due to the effect of alumina. The grain size of the titanomagnetite is around 30 μm, which is relatively large for pillow lavas. Probably the sample is from the core of a large pillow structure in which slow cooling caused large grain sizes.

Irreversible samples from this hole have $T_{c1}$ ranging from 185 to 390°C, $T_{ch}$ from 450 to 575°C, and $J_{ho}/J_o$ from 1.3 to 5.2—similar to samples from Hole 442B. Figure 5 summarizes these results. The irreversible change in magnetization is due to inversion of titanomaghemite (a cubic-spinel phase oxidized at low temperatures) to less-titaniferous magnetite.

### Hole 444A

All igneous rocks recovered from this hole represent massive flows of plagioclase–clinopyroxene–olivine dol-erite. The upper layers, intruded into sediment, contain titanaugite and kaersutite. X-ray-fluorescence analysis indicates that they are alkali olivine basalts (or dolerites), containing more than 6 per cent total alkalis.

Thermomagnetic properties of these samples are all reversible, and their Curie temperatures range between 175 and 445°C (Figure 6). Ilmenite lamellae were recognized in three samples (444A-25-1, 444A-25-3, 444A-27-1) showing a Curie temperature higher than 400°C. The high Curie temperature is caused by low titanium content in the titanomagnetite phase after the formation of ilmenite lamellae. The bulk content of titanium in the opaque minerals is nearly the same as that in the other samples. The $Al_2O_3$ content appears to be higher for this hole than for the other two holes in the Shikoku Basin, but its effect on magnetic properties is unknown.

### Hole 446A

Igneous rocks recovered from this hole represent massive intrusions of alkali-rich plagioclase-clinopyroxene basalts or dolerites. Five of 42 examined samples showed reversible thermomagnetic properties, $T_{c1}$ ranging between 150 and 290°C.

Thermomagnetic properties of thermally irreversible samples are slightly different from those of samples from other holes. Most remarkable is that the Curie temperature after heating $T_{ch}$ is lower than the highest Curie temperature ($T_{c2}$ or $T_{c3}$) revealed in the heating process (Figure 7). $J_{ho}/J_o$ is near unity in irreversible samples.

The apparent decrease in the Curie temperature after heating at 620°C is possibly due to inversion of the ferromagnetic phase having $T_{c2}$ or $T_{c3}$ to non-ferromagnetic ilmenite, as seen in some terrestrial rocks formed by subaerial eruption (Ozima and Larson, 1967). Although the rocks examined in the present study were not formed in a subaerial environment, they appear to have been oxidized at moderately high temperatures. The degree of oxidation in these rocks seems to be great, in spite of the relatively large grain size. The causes of this oxidation of titanomagnetite are unknown. Magnetic miner-

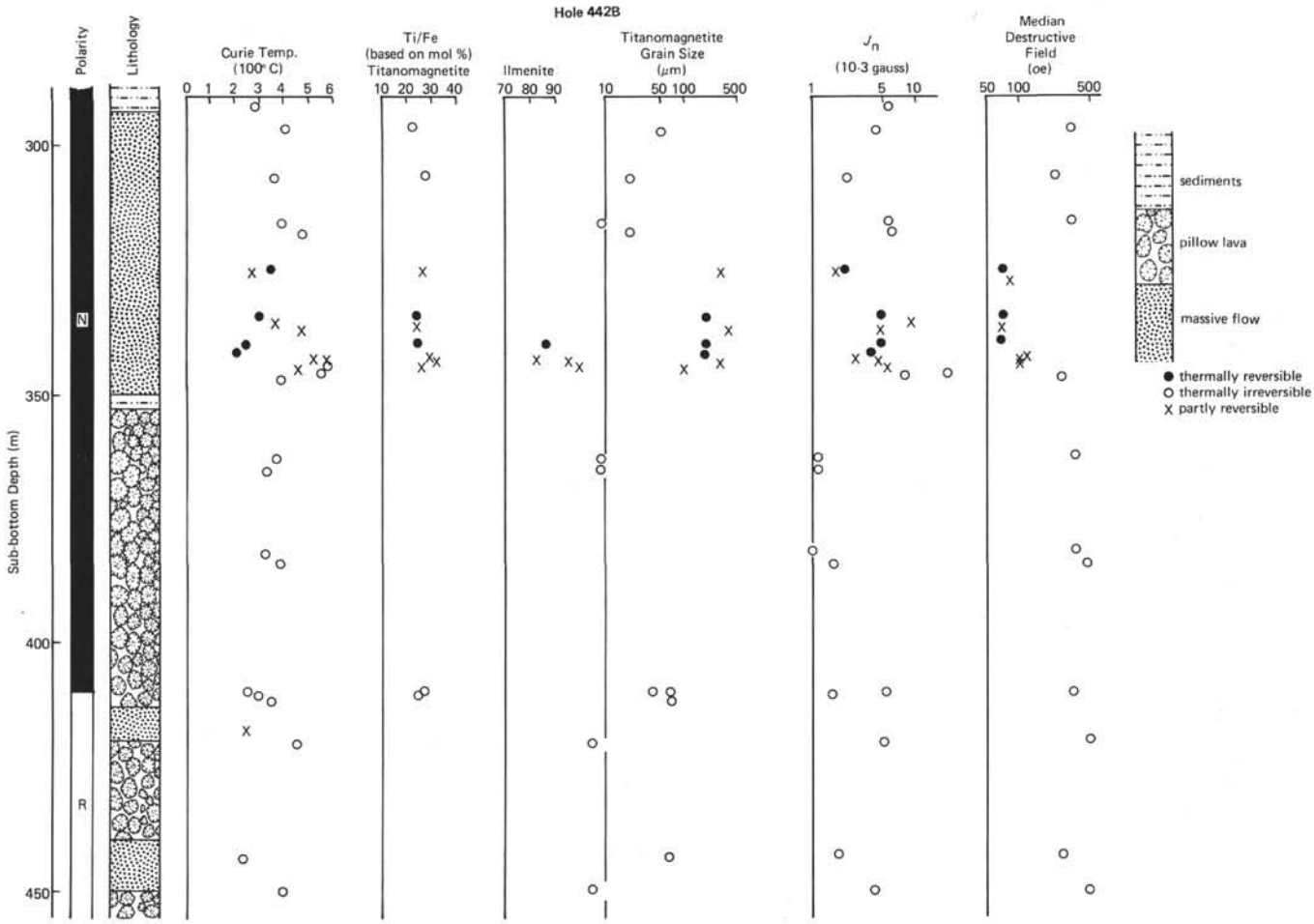


Figure 4. *Down-hole plots of magnetic polarity, lithology, initial Curie temperature, Ti/Fe ratios in titanomagnetite and ilmenite, grain size of titanomagnetite, intensity of natural remanent magnetization ($J_n$) and median destructive field. $J_n$ and MDF taken from Site 442 report.*

als in the intrusive basalts of Hole 444A are almost unoxidized and thermally reversible.

The $Al_2O_3$ content in titanomagnetite in the Hole 446A rocks is 2 to 5.8 weight per cent, nearly twice as high as that for Holes 442B and 443. The $Al_2O_3$ content in titanomagnetite is richer in alkali rocks (446A and 444A) than in tholeiitic rocks (442B and 443).

Because the grain size is sufficiently large, the Ti/Fe ratio of ilmenite coexisting with titanomagnetite was precisely determined by electron microprobe. As seen in Figure 8, there is a positive correlation between Ti/Fe values for titanomagnetite and coexisting ilmenite. Assuming that titanomagnetite and ilmenite were in equilibrium with the environment and with each other during crystallization, the temperature and partial pressure of oxygen during crystallization were 930 to 1150°C and $10^{-13}$ to $10^{-16}$ atm, according to the diagram of Buddington and Lindsley (1964). The Ti/Fe ratio in titanomagnetite increases as secondary oxidation proceeds at low temperatures. The values given above thus may provide only a rough estimate of the crystallization conditions.

## CORRELATION OF THERMOMAGNETIC PROPERTIES WITH LITHOLOGY, MAGNETIC POLARITY AND MAGNETIC INTENSITY

To investigate possible correlations between the magnetochemical characteristics and other properties of rocks, a histogram of initial Curie temperature ($T_{cl}$) was compiled for all samples of massive flows and pillow lavas examined in the present investigation (Figure 9). There seems to be no distinction in $T_{cl}$ between the pillow lavas and massive flows, although the number of pillow-lava samples is insufficient for statistical consideration. Low-temperature oxidation may be controlled by unknown factors, rather than the mode of extrusion.

Figure 10 shows histograms of $T_{cl}$ for normal and reversed magnetic polarities for each hole of Leg 58. No correlation can be recognized between $T_{cl}$ and magnetic polarity, although reversed samples have significantly higher $T_{cl}$ at Hole 446A and generally lower $T_{cl}$ at Holes 442B and 443 than do normal ones. No evidence indicating that the reversed polarity is due to self-reversal has been found.

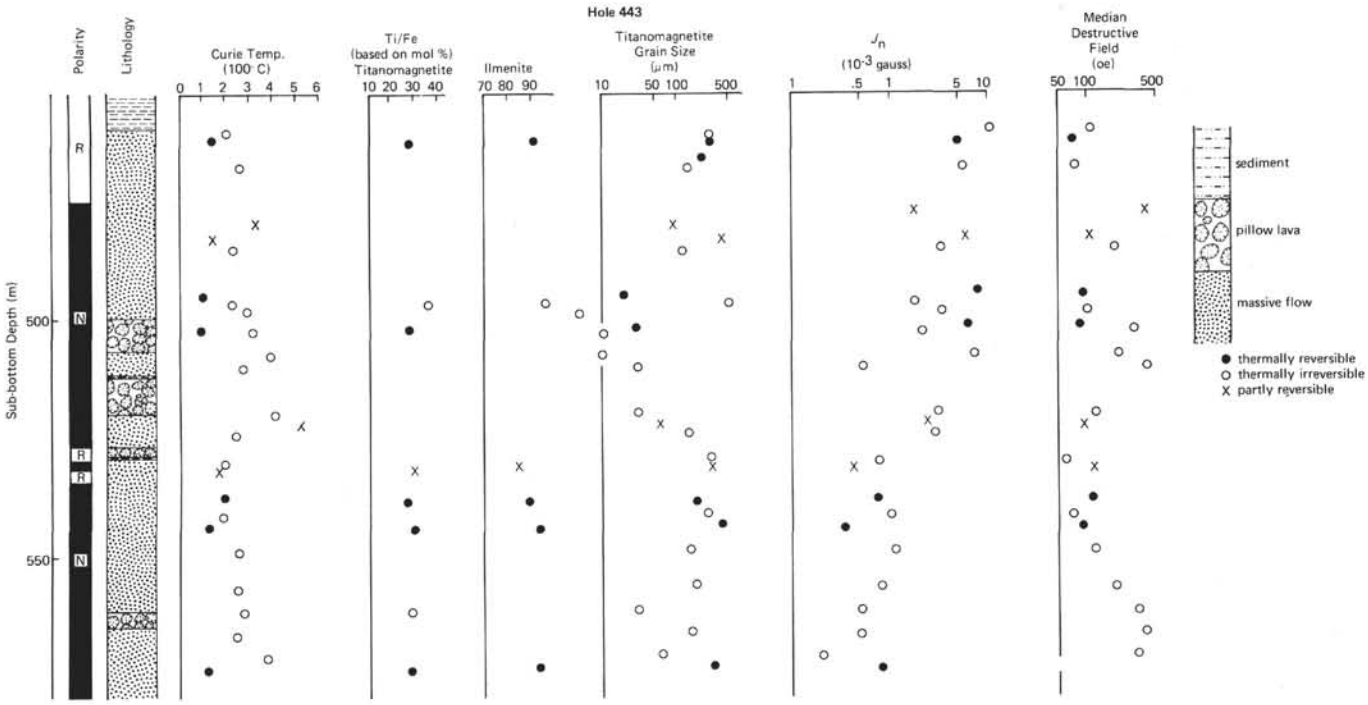


Figure 5. *Down-hole plots of magnetic polarity, lithology, initial Curie temperature, Ti/Fe ratios in titanomagnetite and ilmenite, grain size of titanomagnetite, intensity of natural remanent magnetization ($J_n$), and median destructive field. $J_n$ and MDF taken from Site 443 report.*

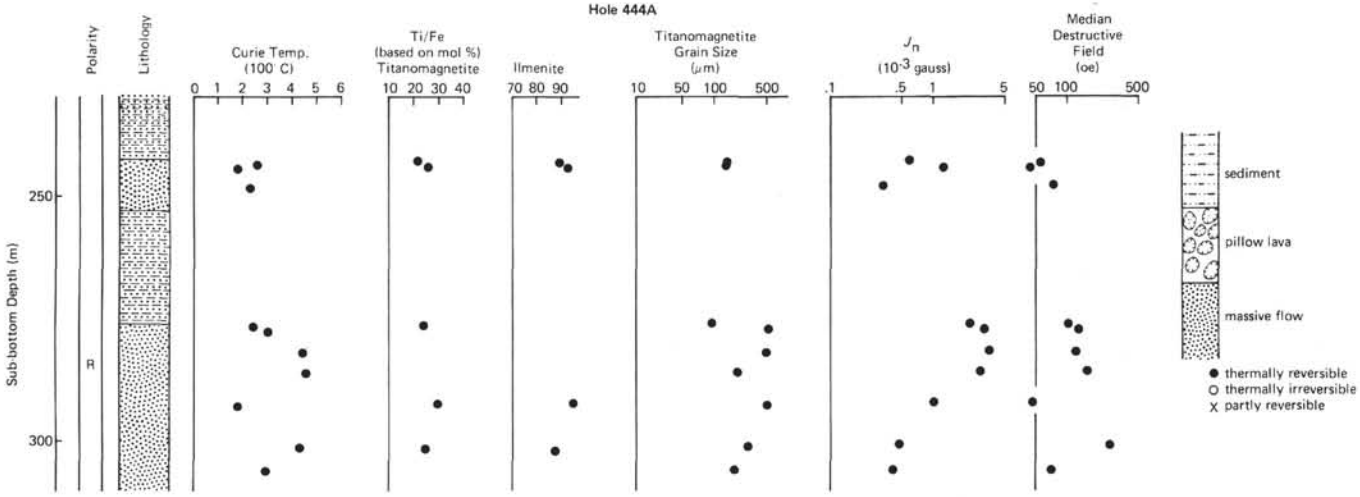


Figure 6. *Down-hole plots of magnetic polarity, lithology, initial Curie temperature, Ti/Fe ratios in titanomagnetite and ilmenite, grain size of titanomagnetite, intensity of natural remanent magnetization ($J_n$), and median destructive field. $J_n$ and MDF taken from Site 444 report.*

The intensity of natural remanent magnetization ($J_n$) of each sample measured on board the *Glomar Challenger* (see site chapters, this volume) is plotted versus the initial Curie temperature in Figure 11. The scatter of values is so large that no correlation is recognized between $J_n$ and $T_{cl}$, although the $T_{cl}$ of a sample having an extremely small $J_n$ is relatively low, and the $T_{cl}$ of a sample having an extremely large $J_n$ is generally high. The values of $J_n$ are not related to the degree of oxidation of titanomagnetite in these samples. Low-temperature oxidation does not seem to systematically alter the intensity of remanent magnetization.

## SUMMARY AND CONCLUSIONS

Comprehensive investigation of magnetic mineralogy of basalt from Leg 58, in combination with shipboard paleomagnetism data for the same samples, suggests the following conclusions:

1. The initial Curie temperature is highly variable, irrespective of site, lithology, or magnetic polarity.

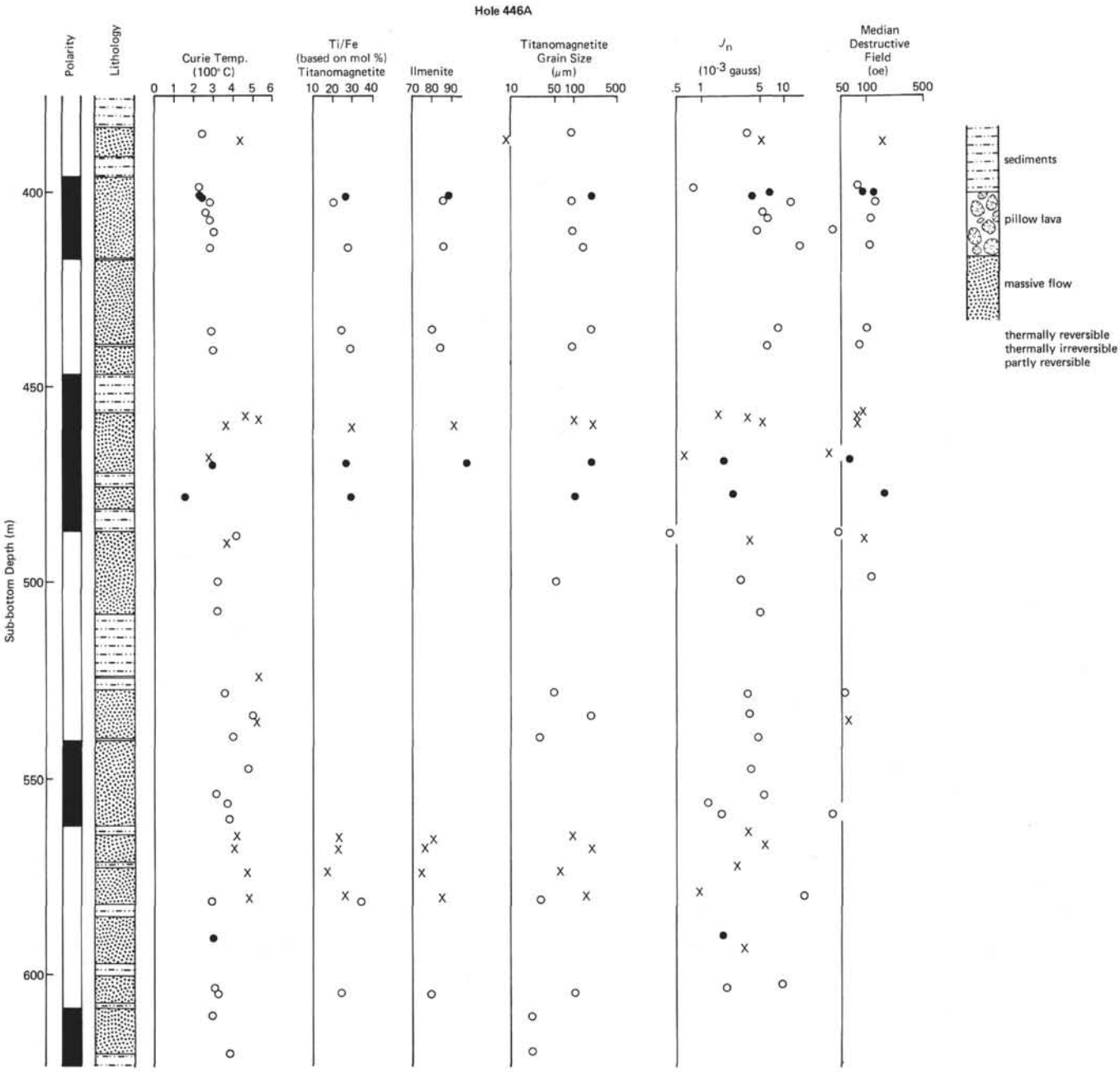


Figure 7. *Down-hole plots of magnetic polarity, lithology, initial Curie temperature, Ti/Fe ratios in titanomagnetite and ilmenite, grain size of titanomagnetite, intensity of natural remanent magnetization ($J_n$), and median destructive field.* $J_n$ *and MDF taken from Site 446 report.*

2. No correlation exists between magnetic polarity and thermomagnetic properties, such as initial Curie temperature and thermal stability. This implies that the reversed magnetization seen in some layers is not due to self-reversal.

3. No correlation exists between intensity of natural remanent magnetization and degree of oxidation.

4. Most of the massive flows cored in Hole 446A seem to have been oxidized at a moderately high temperature, while massive-flow samples from Hole 444A are either unoxidized or oxidized at a higher temperature. Basalts from these two holes appear to have had somewhat different thermal and chemical histories.

5. In rocks from Hole 446A, a systematic correlation is recognized between Ti/Fe ratios of titanomagnetite and coexisting ilmenite. Both minerals seem to have been crystallized at the closing stage of magma solidification. Temperature and oxygen partial pressure during crystallization are estimated at 930 to 1150 °C and $10^{-13}$ to $10^{-16}$ atm, based upon a simplifying assumption.

6. Minor elements in titanomagnetite constitute less than 1 weight per cent, except for $Al_2O_3$, which ranges

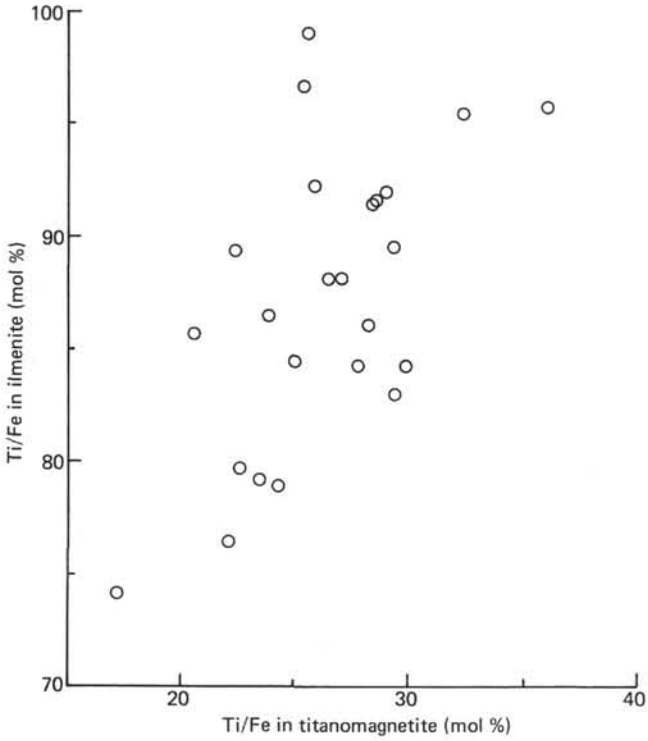


Figure 8. *Ti/Fe ratios in titanomagnetite and ilmenite.*

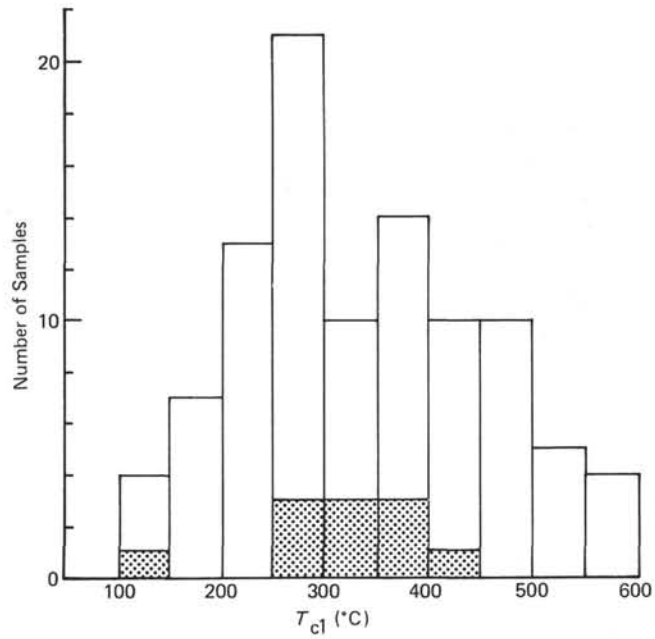


Figure 9. *Histogram of initial Curie temperatures ($T_{c1}$) for all Leg 58 sites. Data from massive basalts (hollow bars) and from pillow lavas (dotted bars) are superposed.*

from 1.0 to 5.8 weight per cent. The $Al_2O_3$ content in titanomagnetite seems to be higher in the alkali basalts.

## ACKNOWLEDGMENTS

We are very grateful to H. Kinoshita and T. Ishii for valuable suggestions and critical reading of this manuscript.

## REFERENCES

Akimoto, S., Katsura, T., and Yoshida, M., 1957. Magnetic properties of $TiFe_2O_4$–$Fe_3O_4$ system and their change with oxidation. *J. Geomagnet. Geoelec.*, 9, 165–178.

Akimoto, S., and Katsura, T., 1959. Magneto-chemical study of the generalized titanomagnetite in volcanic rocks. *J. Geomagnet. Geoelec.*, 10, 69–90.

Buddington, A. F., and Lindsley, D. H., 1964. Iron- titanium oxide minerals and synthetic equivalents. *J. Petrol.*, 5, 318.

Hall, J. M., Fink, L. K., and Johnson, H. P., 1976. Petrography of opaque minerals, Leg 34. *In* Yeats, R. S., Hart, S. R., et al., *Init. Repts. DSDP,* 34: Washington (U.S. Govt. Printing Office), pp. 349–362.

Johnson, J. P., and Hall, J. M., 1978. A detailed rock magnetic and opaque mineralogy study of the basalts from the Nazca Plate. *Geophys. J. Roy. Astron. Soc.*, 197, 45–64.

Kobayashi, K., Steiner, M., Faller, A., Furuta, T., Ishii, T., Shive, P., and Day, R., 1979. Magnetic mineralogy of basalts from Leg 49. *In* Luyendyk, B. P., Cann, J. R., et al., *Init. Repts. DSDP*, 49: Washington (U.S. Govt. Printing Office), pp. 793–805.

Ozima, M., and Larson, E. E., 1967. Study on irreversible change of magnetic properties of some ferromagnetic minerals. *J. Geomagnet. Geoelec.*, 19, 117–128.

_____, 1970. Low- and high-temperature oxidation of titanomagnetite in relation to irreversible changes in themagnetic properties of submarine basalts. *J. Geophys. Res.*, 75, 1003–1018.

Ozima, M., and Ozima, M., and Kaneoka, I., 1968. Potassium-argon ages and magnetic properties of some dredged submarine basalts and their geophysical implications. *J. Geophys. Res.*, 73, 711.

Ozima, M., and Sakamoto, N., 1971. Magnetic properties of synthesized titanomaghemite. *J. Geophys. Res.*, 76, 7035.

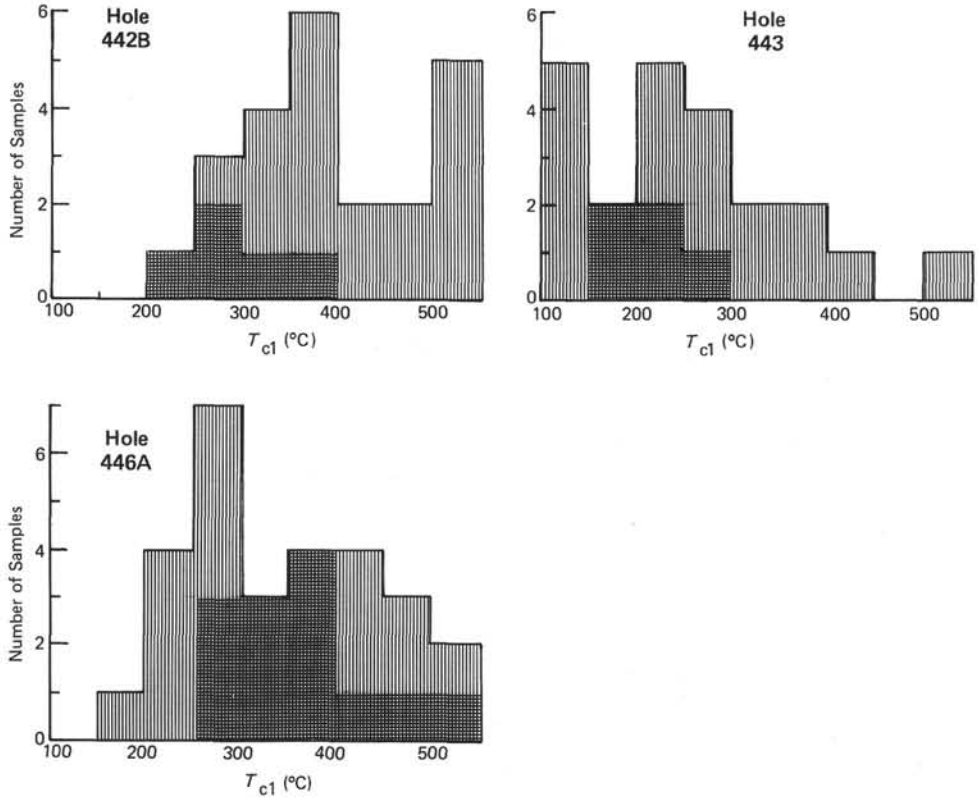


Figure 10. *Histogram of initial Curie temperatures ($T_{cl}$) for all examined rocks. Data from normally magnetized samples (vertically ruled) and from reversely magnetized samples (horizontally ruled) are superposed.*

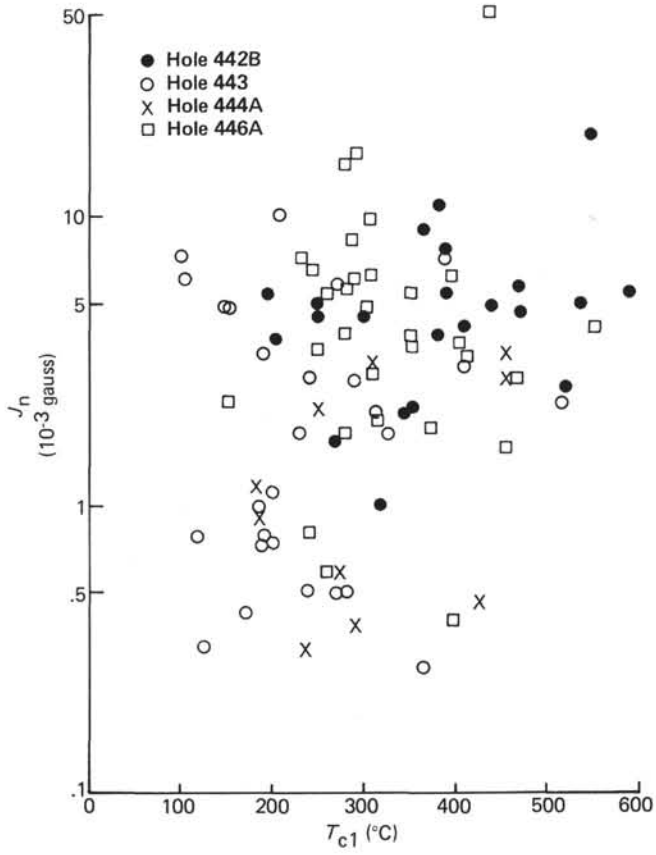


Figure 11. *Relationship between intensity of natural remanent magnetization ($J_n$) and initial Curie temperature ($T_{c1}$).*